Am J Physiol Lung Cell Mol Physiol 303: L75–L87, 2012.
First published May 11, 2012; doi:10.1152/ajplung.00072.2012.

Therapeutic hypercapnia prevents bleomycin-induced pulmonary hypertension in neonatal rats by limiting macrophage-derived tumor necrosis factor-α

A. Charlotte P. Sewing,[1] Crystal Kantores,[1] Julijana Ivanovska,[1] Alvin H. Lee,[1] Azhar Masood,[1,3] Amish Jain,[1,3,4] Patrick J. McNamara,[1,3,4] A. Keith Tanswell,[1,3,4] and Robert P. Jankov[1,2,3,4]

[1]*Physiology and Experimental Medicine Program, Hospital for Sick Children Research Institute, Toronto, Ontario, Canada;* [2]*Heart and Stroke Richard Lewar Centre of Excellence, University of Toronto, Toronto, Ontario, Canada;* [3]*Department of Physiology, University of Toronto, Toronto, Ontario, Canada; and* [4]*Division of Neonatology, Department of Paediatrics, University of Toronto, Toronto, Ontario, Canada*

Submitted 21 February 2012; accepted in final form 2 May 2012

Sewing AC, Kantores C, Ivanovska J, Lee AH, Masood A, Jain A, McNamara PJ, Tanswell AK, Jankov RP. Therapeutic hypercapnia prevents bleomycin-induced pulmonary hypertension in neonatal rats by limiting macrophage-derived tumor necrosis factor-α. *Am J Physiol Lung Cell Mol Physiol* 303: L75–L87, 2012. First published May 11, 2012; doi:10.1152/ajplung.00072.2012.—Bleomycin-induced lung injury is characterized in the neonatal rat by inflammation, arrested lung growth, and pulmonary hypertension (PHT), as observed in human infants with severe bronchopulmonary dysplasia. Inhalation of CO_2 (therapeutic hypercapnia) has been described to limit cytokine production and to have anti-inflammatory effects on the injured lung; we therefore hypothesized that therapeutic hypercapnia would prevent bleomycin-induced lung injury. Spontaneously breathing rat pups were treated with bleomycin (1 mg/kg/d ip) or saline vehicle from postnatal days 1–14 while being continuously exposed to 5% CO_2 (Pa_{CO_2} elevated by 15–20 mmHg), 7% CO_2 (Pa_{CO_2} elevated by 35 mmHg), or normocapnia. Bleomycin-treated animals exposed to 7%, but not 5%, CO_2, had significantly attenuated lung tissue macrophage influx and PHT, as evidenced by normalized pulmonary vascular resistance and right ventricular systolic function, decreased right ventricular hypertrophy, and attenuated remodeling of pulmonary resistance arteries. The level of CO_2 neither prevented increased tissue neutrophil influx nor led to improvements in decreased lung weight, septal thinning, impaired alveolarization, or decreased numbers of peripheral arteries. Bleomycin led to increased expression and content of lung tumor necrosis factor (TNF)-α, which was found to colocalize with tissue macrophages and to be attenuated by exposure to 7% CO_2. Inhibition of TNF-α signaling with the soluble TNF-2 receptor etanercept (0.4 mg/kg ip from *days 1–14* on alternate days) prevented bleomycin-induced PHT without decreasing tissue macrophages and, similar to CO_2, had no effect on arrested alveolar development. Our findings are consistent with a preventive effect of therapeutic hypercapnia with 7% CO_2 on bleomycin-induced PHT via attenuation of macrophage-derived TNF-α. Neither tissue macrophages nor TNF-α appeared to contribute to arrested lung development induced by bleomycin. That 7% CO_2 normalized pulmonary vascular resistance and right ventricular function without improving inhibited airway and vascular development suggests that vascular hypoplasia does not contribute significantly to functional changes of PHT in this model.

carbon dioxide; inflammation; neonatal lung injury

BRONCHOPULMONARY DYSPLASIA (BPD) is a chronic pneumopathy affecting extremely premature infants who frequently require supplemental oxygen and/or mechanical ventilation. The incidence of BPD is inversely proportional to the gestational age at which infants are born, with an incidence approaching 60% in the smallest survivors (4). The cardinal feature of BPD, as observed in the current era, is an inhibition or arrest of alveolar and vascular growth (29). The underlying pathogenesis of BPD appears to be multifactorial, but upregulation of inflammatory mediators leading to, or caused by, infiltration of inflammatory cells, including macrophages and neutrophils, is believed to play a major role (61, 62, 66). Pulmonary hypertension (PHT) is common in those infants that are most severely affected (15, 58, 67), which signals greatly increased morbidity and mortality related, in major part, to consequent right heart failure (33). Putative factors contributing to progressive and fatal PHT in BPD include sustained vasoconstriction, arterial wall remodeling, and pruning of peripheral resistance arteries (58), but the upstream mediators and relative contributions of these changes to chronically increased pulmonary vascular resistance (PVR) and right ventricular dysfunction remain poorly understood.

Management strategies employed in an attempt to prevent or ameliorate BPD have thus far met with limited success but include avoidance or minimization of mechanical ventilation and high inspired O_2 concentrations to reduce the potential for volutrauma and oxygen toxicity (1). With avoidance of excessive mechanical ventilation has come a necessary shift in clinical practice towards "permissive hypercapnia" (acceptance of "higher-than-normal" Pa_{CO_2} levels) becoming the norm (28), although evidence of the effectiveness in reducing the incidence and severity of BPD remains lacking (76). Possible explanations for a lack of benefit in clinical trials (49) may be that the target Pa_{CO_2} was less than required or that harmful effects of hypoventilation and small tidal volumes in the suboptimally recruited lung may have counteracted any benefit. Despite ongoing uncertainty about the utility of permissive hypercapnia in the neonate (35), there is growing experimental evidence to indicate that inhaled or exogenous CO_2 (so-called "therapeutic hypercapnia") may protect the lung from diverse injuries, including those secondary to systemic ischemia reperfusion (38), endotoxin (37, 72), high tidal volume mechanical ventilation (7, 65, 69), and chronic exposure to hyperoxia (45) or hypoxia (31, 56). Putative mediators of lung injury shown to be attenuated by therapeutic hypercapnia in these models have included inflammatory cell influx (37, 45, 72), proinflammatory cytokines (14, 38, 72), and oxidative stress (31, 38, 52, 72). However, several studies have also indicated the potential for hypercapnia to worsen lung injury (41, 53, 54) and to potentially cause an increase in inflammation in the

Address for reprint requests and other correspondence: R. P. Jankov, Physiology and Experimental Medicine Program, Hospital for Sick Children Research Institute, 555 Univ. Ave, Toronto, Ontario, Canada M5G 1X8 (e-mail: robert.jankov@sickkids.ca).

noninjured lung (2, 45), highlighting the need for further study. Our aim therefore was to examine effects of therapeutic hypercapnia in a new rat model with similarities to human BPD (47), secondary to bleomycin exposure.

Bleomycin sulfate is a chemotherapeutic agent that produces a dose-dependent pulmonary inflammatory and fibrotic response in humans when administered systemically and in adult rodents when instilled as a single intratracheal dose (32) or by repeated intraperitoneal injection (6). The early phases of bleomycin-induced lung injury are characterized by increased expression of proinflammatory cytokines (19), a marked inflammatory cell influx that is dominated by macrophages (27), increased apoptosis (20), changes in growth factors, such as transforming growth factor-β (3, 12), "emphysematous" lung morphology, and severe PHT (63, 77). In neonatal rats, selective decrease in lung growth, arrested alveolarization and vascular hypoplasia are prominent features (47, 74). Herein, we report that exposure to CO_2 led to dose-dependent preventive effects on bleomycin-induced PHT without affecting lung growth, arrested alveolarization, or vascular hypoplasia. Tumor necrosis factor (TNF)-α was found to be increased by bleomycin and to colocalize with tissue macrophages, both of which were attenuated by 7% CO_2. Inhibition of TNF-α signaling with a soluble TNF-2 receptor, etanercept, also prevented the hemodynamic and structural changes of chronic PHT, suggesting that the benefits of CO_2 on the pulmonary vasculature were mediated, in major part, via this pathway.

MATERIALS AND METHODS

Materials. Bleomycin sulfate was purchased from Calbiochem (San Diego, CA). Etanercept (Enbrel) was from Amgen (Thousand Oaks, CA). Plexiglas animal exposure chambers and automated O_2/CO_2 controllers were from BioSpherix (Lacona, NY). Acids, alcohols, organic solvents, paraformaldehyde, Permount, and Superfrost/Plus microscope slides were from Fisher Scientific (Whitby, ON, Canada). DMEM, trypsin, and FBS were from Wisent Bioproducts (St-Bruno, Quebec, Canada). Avidin-biotin-peroxidase complex immunohistochemistry kits, 3, 3′-diaminobenzidine staining kits, DAPI fluorescent mounting medium, and normal goat serum were from Vector Laboratories (Burlingame, CA). Weigert's resorcin-fuchsin stain was from Rowley Biochemical (Danvers, MA). Terminal deoxyuridine triphosphate (dUTP) nick-end labeling (TUNEL) assay kits were from Roche (Laval, Québec, Canada). Alexa Fluor 488-conjugated isolectin B_4 (cat no. I21411), derived from *Griffonia Simplicifolia*, Alexa Fluor 488-conjugated goat anti-mouse (cat no. A-10680), and AlexaFluor 546-conjugated anti-goat secondary antibody (cat no. A-11056) were from Life Technologies (Burlington, ON, Canada). Anti-glyceraldehyde-3-phosphate dehydrogenase (GAPDH; cat no. sc-25778), anti-tumor necrosis factor (TNF)-α (cat no. sc-1349, used for fluorescent immunostaining), and goat anti-rabbit and -mouse IgG-biotin antibodies were from Santa Cruz Biotechnology (Santa Cruz, CA). Anti-cluster of differentiation (CD)68 (cat no. MCA341R) was from Serotec (Raleigh, NC). Anti-myeloperoxidase (MPO; cat no. A0398) was from DAKOCytomation (Mississauga, ON, Canada). Anti-TNF-α (cat no. HP8001, used for Western blotting) was from Hycult Biotech (Uden, The Netherlands). Goat anti-rabbit and anti-mouse IgG-peroxidase antibodies were from Cell Signaling Technology (Beverly, MA). Unless otherwise specified, all other chemicals and reagents were from Bioshop Canada (Burlington, ON, Canada).

Animal exposures and interventions. All procedures involving animals were performed in accordance with the standards of the Canadian Council on Animal Care and were approved by the Animal Care Committee of the Hospital for Sick Children Research Institute. Commencing on the day after birth, pups received bleomycin sulfate 1 mg/kg in 0.9% saline (5 μl/g body wt by 27-G needle in the right iliac fossa) or 0.9% saline (vehicle control) daily intraperitoneally for 14 days, as previously described (47), while being concurrently exposed to either normocapnia (< 0.5% environmental CO_2) or 5% or 7% CO_2 (O_2 21%, balance N_2) (31). In separate experiments, bleomycin-exposed pups received an additional intraperitoneal injection of etanercept (0.4 mg/kg in 0.9% saline; 5 μl/g body wt ip) on alternate days commencing on postnatal *day 1*. The dose of etanercept used was the same as that recently described to be effective in preventing PHT in monocrotaline-exposed adult rats (71). Each litter was maintained at $n = 10–12$ pups to control for nutritional effects. At the end of each 14-day exposure period, pups were either killed by pentobarbital overdose or exsanguinated after anesthesia.

Arterial blood gas measurement. Pups were lightly anesthetized with ketamine (40 mg/kg ip) and xylazine (6 mg/kg ip), and the neck was dissected to expose the external carotid artery. After a 15-min recovery, while the animals breathed the appropriate concentrations of CO_2, the artery was transected and blood was immediately collected with a heparinized capillary tube and analyzed (ABL800; Radiometer, Copenhagen, Denmark).

Cardiac ventricular weights, lung wet/dry weights, and brain weight. Right ventricular hypertrophy (RVH) was quantified by measuring the right ventricle (RV) to left ventricle and septum (LV + S) weight ratio (Fulton index), as previously described (25). Lung wet-to-dry weight ratio was determined by measuring left lung weight immediately upon harvest and again following baking at 65°C for 48 h. Brain wet weight included the cortex and cerebellum only after removal of the brainstem and spinal cord.

Two-dimensional echocardiography-derived measurements of pulmonary hemodynamics. Pulmonary hemodynamics were evaluated noninvasively using two-dimensional echocardiography and Doppler ultrasound (Vivid 7 cardiac ultrasound system and I13L linear probe; GE Medical Systems, Milwaukee, WI), as previously described in detail (31, 47). Animals were lightly anesthetized with ketamine/xylazine and spontaneously breathing at the time of the study. For estimation of PVR, a short axis view at the level of the aortic valve was obtained and the pulmonary artery was identified by color flow Doppler. The pulmonary arterial acceleration time (PAAT) was measured as the time from the onset of systolic flow to peak pulmonary outflow velocity and the RV ejection time (RVET) as the time from onset to completion of systolic pulmonary flow. Pulmonary vascular resistance was estimated using the formula: RVET/PAAT. For estimation of RV stroke volume, the PA diameter was measured by color flow Doppler at the hinge point of the pulmonary valve leaflets. From the same Doppler interrogation of the pulmonary artery used to measure PAAT and RVET, RV output was calculated using the formula: $(\text{PA diameter}/2)^2 \times 3.14 \times$ PA velocity time integral $\times$ heart rate (beats/min). The PA velocity time integral was measured by tracing the leading edge of the velocity time graph from the onset to completion of systolic pulmonary flow. RV output (ml/min) was corrected for body weight to derive a RV performance index (RVI; $\text{ml}\cdot\text{min}^{-1}\cdot\text{kg}^{-1}$). Left ventricular (LV) shortening fraction was measured from the parasternal short axis view according to the formula: [(LV end-diastolic diameter − LV systolic diameter)/LV end-diastolic diameter] × 100.

Histological studies. Lungs from four animals from each group (2 from each of 2 separate litters) were air inflated and perfusion fixed at a constant pressure, embedded in paraffin, sectioned, immunostained for CD68 (to identify macrophages) and myeloperoxidase (MPO; to identify neutrophils), and stained with hematoxylin and eosin, or for elastin, as previously described (31, 45, 57). Paraffin-embedded cortical brain sections (5 μm) were labeled for apoptotic nuclei using a commercially available fluorescein TUNEL enzymatic assay kit (Roche).

Table 1. *Rat primer sequences for quantitative PCR*

Gene (RefSeq Accession No.)	Forward 5′-3′	Reverse 5′-3′
β-Actin (NM_031144)	CTGGGTATGGAATCCTGTGG	TAGAGCCACCAATCCACACA
CCL2 (MCP-1) (NM_031530)	CTGTAGCATCCACGTGCTGT	TGAGGTGGTTGTGGAAAAGA
CCL3 (MIP-1α) (NM_013025)	CCACCGCTGCCCTTGCTGTT	CACCCGGCTGGGAGCAAAGG
CCL4 (MIP-1β) (NM_053585)	CTCTCTCCTCCTGCTTGTGG	CACAGATTTGCCTGCCTTTT
CCL5 (RANTES) (NM_031116)	CTGCTGCTTTGCCTACCTCT	CGAGTGACAAAGACGACTGC
CCL7 (MCP-3) (NM_001007612)	AACCAGATGGGACCAATTCA	CACAGACTTCCATGCCCTTT
CCR1 (NM_020542)	ACCTGTTCAACCTGGCTGTC	AGGGAAAACACTGCATGGAC
CCR2 (NM_021866)	CTGCCCCTACTTGTCATGGT	GGCCTGGTCTAAGTGCATGT
CCR3 (NM_053958)	CAGCAGAGCATACACCTGGA	CGCCAGGAAGGAATGAAATA
CCR5 (NM_053960)	AAAGTCTGGCAATGGTGAGC	CTCCCAGTAAACCTCCCACA
CXCL1 (CINC-1) (NM_030845)	AGACAGTGGCAGGGATTCAC	GGGGACACCCTTTAGCATCT
CXCL2 (MIP-2α) (NM_053647)	ACCAACCATCAGGGTACAGG	GGCTTCAGGGTTGAGACAAA
CXCR1 (NM_019310)	GCTATGAGGTCCTGGGTGAA	GAGTGTCCGAGAGCAGAACC
CXCR2 (NM_017183)	GATTCTTGGCTTCCTCCACA	GGAGGTGTTCGCTGAAGAAG
GAPDH (NM_017183)	CCATGTTTGTGATGGGTGTG	GGCATGGACTGTGGTCATGA
Interleukin-1α (NM_022194)	TCGGGAGGAGACGACTCTAA	GAAAGCTGCGGATGTGAAGT
Interleukin-1β (NM_017008)	CTGTGACTCGTGGGATGATG	GGGATTTTGTCGTTGCTTGT
Interleukin-1 Receptor Antagonist (NM-017019)	GAAAAGACCCTGCAAGATGC	GATGCCCAAGAACACATTCC
Interleukin-6 (NM_012589)	GCCAGAGTCATTCAGAGCAA	GGTTTGCCGAGTAGACCTCA
Tumor necrosis factor-α (NM_012675)	CAGCAGATGGGCTGTACCTT	CTGGAAGACTCCTCCCAGGT
Tumor necrosis factor receptor-1 (NM_013091)	GTCAAAGAGGTGGAGGGTGA	TTACAGGTGGCACGAAGTTG
Tumor necrosis factor receptor-2 (NM_130426)	GTCATCCCCAAGCAAGAGTC	CATCCTTTGGAGACCCTGAA

Morphometric analyses. For all analyses, measurements were carried out on four left lung sections per animal and four animals (representing 2 litters) per treatment group by observers blinded to group identity. For assessment of percentage arterial medial wall thickness (%MWT), pulmonary arteries were identified by the presence of both inner and outer elastic lamina using Hart's elastin stain, as previously described in detail (31). Analyses of tissue macrophage (CD68-positive) and neutrophil (MPO-positive) cell numbers and distal airway structure, including mean linear intercept (MLI; using hematoxylin and eosin-stained sections), tissue fraction (hematoxylin and eosin), secondary crest numbers (identified by positive staining for elastin at their tips), and counts of peripheral arteries (identified as vessels of external diameter between 20 and 65 μm with both internal and external elastic laminae visible) were conducted as previously described in detail (44, 45, 57) from 10 random nonoverlapping fields captured from each section.

Staining of frozen sections. Lungs were inflated and snap frozen in optimum cutting temperature compound, as previously described (22) and then cut by cryostat in to 10-μm sections, which were mounted and stored at −80°C until analysis. Slides were fixed in ice-cold acetone and incubated with Isolectin B_4 (diluted 1:100), according to the manufacturer's instructions, known to label "stimulated" or classically activated macrophages by binding to cell membrane glycoconjugates bearing terminal α-D-galactose (42). For colabeling studies, anti-CD68 and -TNF-α were applied (both diluted 1:50, 1 h at room temperature), followed by appropriate secondary antibodies (each diluted to 1:300 with blocking solution, at room temperature in the dark for 30 min), before aqueous mounting with DAPI. Images were digitally captured using an epifluorescent microscope with appropriate filter sets. Identical images acquired with different filter sets were merged using Image-Pro Plus software (version 7.0, Media Cybernetics, Bethesda, MD).

Quantitative PCR. RNA was extracted (Absolutely RNA Miniprep kit; Agilent/Stratagene, La Jolla, CA) and reverse transcribed (AffinityScript; Agilent) from lung tissue samples stored in RNALater (Applied Biosystems, Streetsville, ON, Canada). Quantitative (q)PCR was performed on a Stratagene MX3000P qPCR system using SYBR Green qPCR Master Mix (SA Biosciences, Frederick, MD). Cycling conditions were 95°C for 10 min followed by 40 cycles of 95°C for 15 s and 60°C for 60 s. A standard curve for each primer set was run, using a rat lung cDNA standard (Agilent), to ensure that reaction efficiency was equivalent to primers for housekeeping genes. Primer sequences are listed in Table 1. A dissociation curve was run for each set of samples to exclude nonspecific product formation and reaction contamination. Samples were run in duplicate, and expression of the gene of interest, where reported, was normalized to β-actin and GAPDH. Fold or fraction change in expression relative to control samples was calculated by the $2^{-\Delta\Delta Ct}$ method using Stratagene MxPro software (v 4.01).

Western blot analyses. Lung tissues from four animals per group (2 from each of 2 separate litters) were lysed in RIPA buffer containing protease inhibitors, fractionated by SDS-PAGE, transferred to poly-

Table 2. *Body weight, lung weight and arterial blood gas values on day 14*

Parameter/Group	Vehicle + Normocapnia	Bleomycin + Normocapnia	Vehicle + 5% CO_2	Bleomycin + 5% CO_2	Vehicle + 7% CO_2	Bleomycin + 7% CO_2
BW, g	28.7 ± 1.2	29.5 ± 1.8	31.3 ± 2.3	28.5 ± 1.4	30.0 ± 1.9	27.6 ± 1.6
LW, mg	517 ± 39	360 ± 24*	490 ± 41	375 ± 31*	534 ± 33	318 ± 37*
LW/BW × 10^3	18.3 ± 0.3	12.5 ± 0.4*	16.0 ± 0.03	12.9 ± 0.02*	17.8 ± 0.04	12.1 ± 0.05*
pH	7.33 ± 0.03	7.30 ± 0.06	7.30 ± 0.03	7.32 ± 0.01	7.20 ± 0.02†	7.20 ± 0.04†
Pa_{CO_2}, mmHg	49.0 ± 4.1	55.5 ± 9.1	62.2 ± 7.1	72.5 ± 4.2†	80.2 ± 4.8†	90.5 ± 8.0†
Pa_{O_2}, mmHg	69.9 ± 6.5	56.8 ± 13.4	128.9 ± 9.4†	103.1 ± 5.3†	159.1 ± 46†	131.2 ± 15.8†
HCO_3^-, mmol/l	25.7 ± 0.9	24.1 ± 1.8	29.7 ± 1.1†	36.1 ± 1.7‡	29.7 ± 1.2†	29.9 ± 3.1†

Values represent means ± SD; $n = 8$–20 animals per group for weight data and 5–8 animals per group for blood gas data. LW, lung weight; BW, body weight. *$P < 0.01$, by ANOVA, compared with respective vehicle-treated group. †$P < 0.05$, by ANOVA, compared with normocapnia-exposed groups. ‡$P < 0.01$, by ANOVA, compared with all other groups.

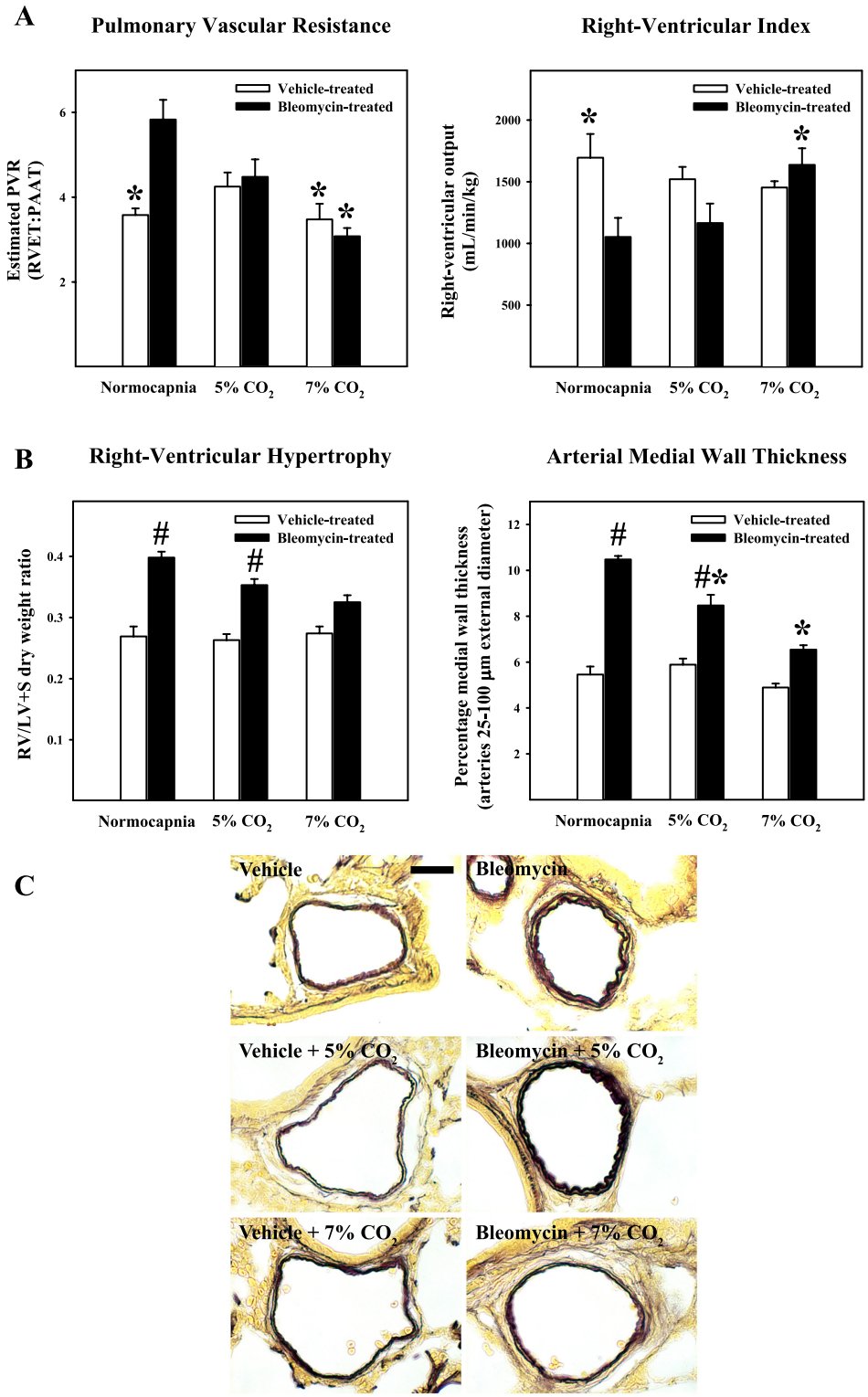

Fig. 1. Exposure to 7% CO_2 prevents bleomycin-induced pulmonary hypertension. Pups were treated from postnatal *days 1–14* with vehicle (open bars) or bleomycin (1 mg·kg^{-1}·day^{-1}; closed bars) while receiving concurrent exposure to normocapnia (< 0.5%) or 5% or 7% CO_2. All values represent means ± SE. *A*: pulmonary vascular resistance (PVR; *left*), as estimated by the right ventricular ejection time (RVET)/pulmonary arterial acceleration time (PAAT) ratio and right ventricular index (*right*), as a marker of right-ventricular systolic function (n = 6–8 animals/group). *B*: right ventricle (RV)/left ventricle + septum (LV + S) dry weight ratios as a marker of RV hypertrophy (n = 10–12 animals/group) and percent arterial medial wall thickness (n = 4 animals/group) as a marker of pulmonary arterial remodeling. *P < 0.01, by ANOVA, compared with bleomycin-treated normocapnia-exposed group. #P < 0.01, by ANOVA, compared with vehicle-treated groups. *C*: representative photomicrographs of elastin staining (dark brown inner and outer elastic laminae delineating the medial vascular wall; bar length = 25 μm) demonstrating medial wall thickening in bleomycin-exposed animals (bleomycin), which was largely prevented by concurrent exposure to 7% CO_2 (bleomycin + 7% CO_2).

vinylidene difluoride membranes, and blotted, and band densities were measured as previously described (23). Differences in protein loading were compensated for by reblotting for GAPDH, the expression of which was found, in preliminary studies, to be unaffected by chronic exposure to bleomycin or to CO_2. Dilutions of primary antisera were 1:200 for TNF-α and 1:5,000 for GAPDH. Protein bands were identified using enhanced chemiluminescent substrate (Immobilon; Millipore), and images were digitally captured using a MicroChemi chemiluminescent image analysis system (DNR Bioimaging Systems, Jerusalem, Israel). Bands were quantified by digital densitometry of nonsaturated images with background density removed (ImageJ, NIH, Bethesda, MD).

Data presentation and analysis. All values are expressed as means ± SE. Statistical significance (P < 0.05) was determined by one-way ANOVA followed by pair-wise multiple comparisons using the Tukey test (SigmaStat; Systat Software, San Jose, CA).

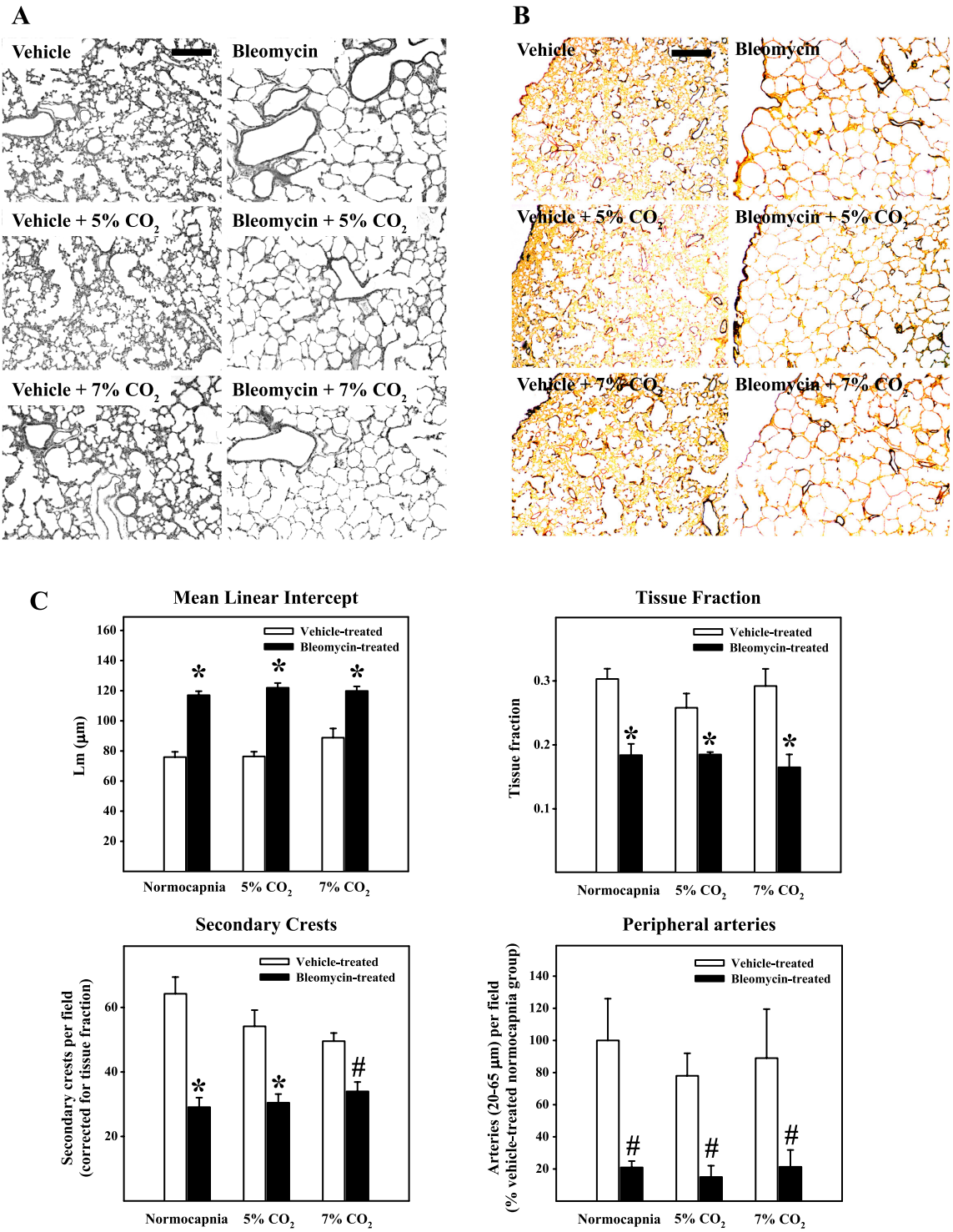

Fig. 2. Exposure to CO_2 does not improve abnormal distal airway morphology. Pups were treated from postnatal *days 1–14* with vehicle (open bars) or bleomycin (1 mg·kg^{-1}·day^{-1}; closed bars) while receiving concurrent exposure to normocapnia (< 0.5%) or 5% or 7% CO_2. Representative low-power photomicrographs of hematoxylin and eosin-stained sections (*A*) demonstrating marked distal airway simplification and septal thinning in bleomycin-treated animals and elastin-stained sections (*B*) demonstrating a marked decrease in numbers of small peripheral arteries (outlined by dark brown stain for elastin) in bleomycin-treated animals, both of which were unaffected by exposure to CO_2. Bar lengths = 200 μm. *C*: morphometric analyses of mean linear intercept (Lm), tissue fraction, and secondary crests or peripheral arteries per field, corrected for tissue fraction. Values represent means ± SE for $n = 4$ animals/group. *$P <$ 0.01, by one-way ANOVA, compared with respective vehicle-treated groups. #$P < 0.05$, by one-way ANOVA, compared with respective vehicle-treated group.

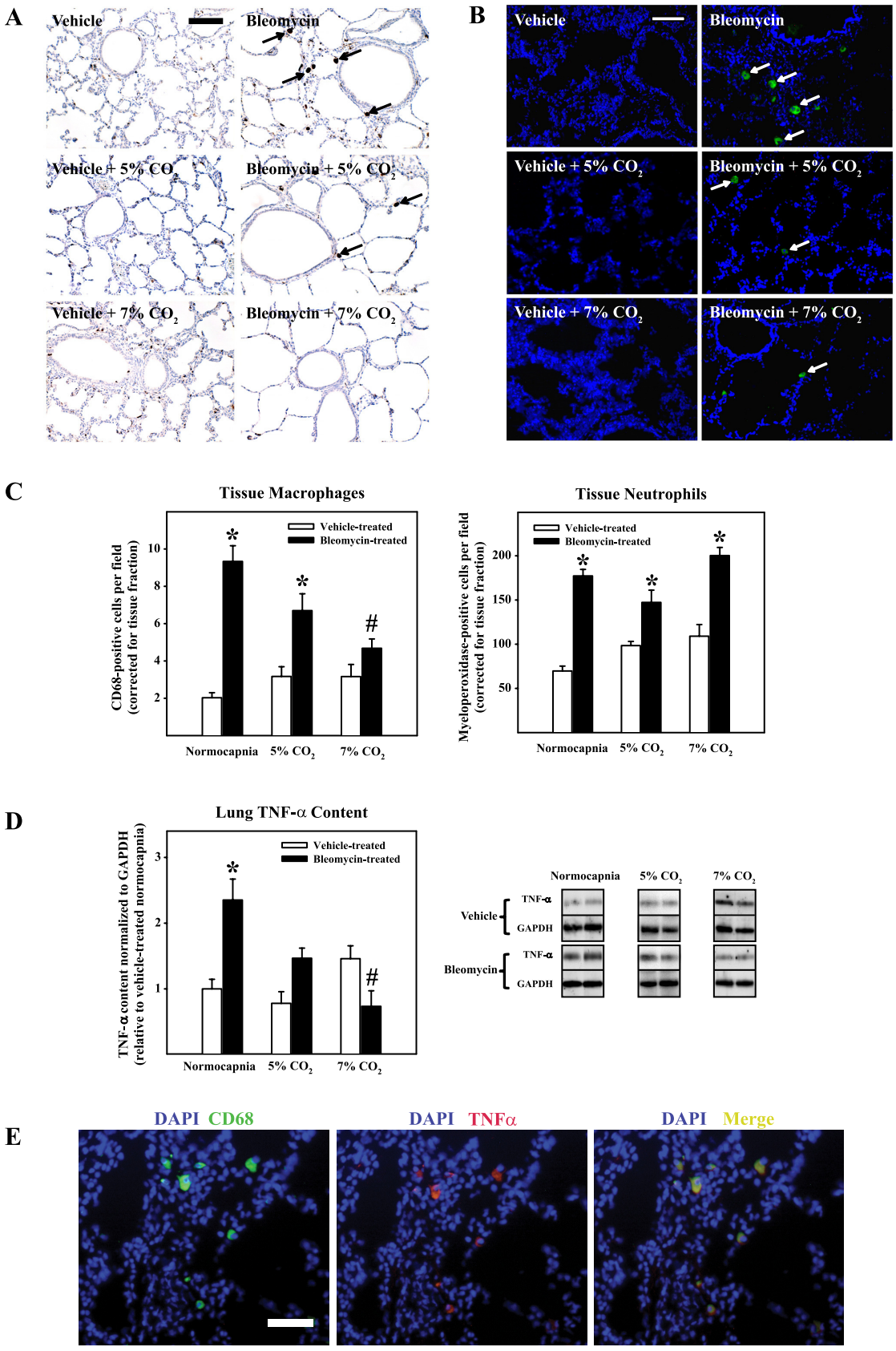

RESULTS

Body weights, lung weights, and arterial blood gas measurements. Values are shown in Table 2. Neither treatment with bleomycin nor exposure to either level of CO_2 for 14 days had any significant effect on body weight, relative to vehicle-treated or normocapnia-exposed controls. In contrast, lung weights and lung weight-to-body weight ratios were significantly decreased in bleomycin-treated animals, whether or not they were exposed to CO_2. Treatment with bleomycin and/or exposure to CO_2 had no significant effects on lung wet/dry weight ratios ($P > 0.5$; data not shown). Exposure of bleomycin-treated animals to 5% CO_2 increased Pa_{CO_2} by ~ 15–20 mmHg and exposure to 7% CO_2 by ~ 35 mmHg above levels measured in normocapnia-exposed controls. Only exposure to 7% CO_2 caused significant persistent acidosis at 14 days due to partial metabolic correction, as reflected in lower pH and higher HCO_3^- HCO_3 levels than normocapnic controls, whereas animals exposed to 5% CO_2 had evidence of complete metabolic correction by *day 14*. Interestingly, and as previously reported in hypoxia-exposed animals (31), exposure to either level of CO_2 significantly increased Pa_{O_2} in both vehicle- and bleomycin-treated animals.

Effects of CO_2 on abnormal pulmonary hemodynamics. To distinguish acute from chronic effects of hypercapnia, preliminary measurements were first obtained while animals continued to breathe CO_2 and were repeated following a 15-min period of recovery in room air. PVR index was found to be unchanged ($P > 0.5$ by ANOVA; data not shown) by removal from CO_2; therefore, all reported data were obtained while animals were breathing room air. As previously reported (47), treatment with bleomycin for 14 days led to a significantly increased the PVR index (Fig. 1*A*, *left*) and decreased RVI (Fig. 1*A*, *right*), relative to vehicle-treated controls. Bleomycin-induced increase in PVR index and decrease in RVI were normalized by exposure to 7% CO_2 (Fig. 1*A*), whereas exposure to 5% CO_2 had no significant effect ($P > 0.05$). Neither treatment with bleomycin, nor exposure to CO_2, caused any significant change in LV fractional shortening ($P > 0.5$ by ANOVA; data not shown).

Effects of CO_2 on structural changes of pulmonary hypertension. As previously reported (47), treatment with bleomycin for 14 days led to significant RVH (Fig. 1*B*) and increased %MWT (Fig. 2*B*) in pulmonary resistance arteries. Exposure to 7% CO_2 significantly ($P < 0.05$) attenuated RVH (Fig. 2*A*) and %MWT in bleomycin-treated animals (Fig. 1*B*). Exposure to 5% CO_2 caused no change in RVH ($P > 0.05$) and a smaller, but significant ($P < 0.05$) decrease in %MWT (Fig. 1*B*). Relative differences in medial wall thickness between groups are illustrated by high-power images of elastin-stained pulmonary arteries (Fig. 1*C*).

Table 3. *Changes in mRNA expression secondary to bleomycin*

Gene	Bleomycin	Vehicle + 7% CO_2	Bleomycin + 7% CO_2
CXCL1	9.7 ± 2.4*	2.7 ± 0.5*	13.3 ± 1.7*
CXCR1	2.3 ± 0.2*	2.4 ± 0.3*	2.1 ± 0.2
Tumor necrosis factor-α	2.3 ± 0.3*	1.3 ± 0.1	1.0 ± 0.2

Values are means ± SE of 4 samples *per* group relative to control (vehicle-treated normocapnia-exposed) group, which was assigned a value of 1. *$P < 0.05$, by ANOVA, compared with control.

Changes in distal airway morphology secondary to bleomycin. As shown in representative low-power hematoxylin and eosin-stained sections (Fig. 2*A*) and by low-power elastin-stained sections (Fig. 2*B*), the lung structure of bleomycin-treated animals was characterized by septal thinning, arrested alveolarization (manifesting as "emphysematous" distal airspaces), and vascular rarefaction as quantified by increased MLI and by decreased tissue fraction, secondary crest counts and peripheral artery counts (Fig. 2*C*). Neither level of CO_2 had any effects on these changes in either vehicle- or bleomycin-treated animals (Fig. 2*C*).

Effects of CO_2 on tissue inflammatory cells. As illustrated by CD68 immunostaining (Fig. 3*A*) and by isolectin B_4 binding (Fig. 3*B*), large classically activated macrophages were present in greatly increased numbers in the lungs of animals treated with bleomycin for 14 days (Fig. 3C). Concurrent exposure to 7% CO_2 significantly ($P < 0.05$) attenuated macrophage numbers in the bleomycin-treated lung, whereas 5% CO_2 had no significant effect ($P > 0.05$; Fig. 3*C*). As also shown in Fig. 3*C*, treatment with bleomycin led to significantly ($P < 0.05$) increased numbers of MPO-positive neutrophils, which were unaffected by exposure to either level of CO_2. Changes in expression of proinflammatory cytokines and chemokines (listed in Table 1) were screened by qPCR on *day 14*. Genes for which significant ($P < 0.05$) changes were found are listed in Table 3. The neutrophil chemokine CXCL1 (also known as CINC-1) and its receptor, CXCR1, were greatly increased by bleomycin but were unaffected by exposure to 7% CO_2 (Table 3). TNF-α, a proinflammatory cytokine that may recruit macrophages to the lung (18, 46) or be tissue macrophage derived (59), was increased in bleomycin-exposed lungs and was normalized by concurrent exposure to 7% CO_2 (Table 3). Similar to findings in qPCR, lung TNF-α protein content was significantly ($P < 0.05$) increased by treatment with bleomycin and completely normalized by exposure to 7%, but not by 5%, CO_2 (Fig. 3*D*). Double labeling for immunoreactive CD68 and TNF-α in lungs of bleomycin-treated animals revealed that TNF-α colocalized with macrophages (Fig. 3*E*), implicating

Fig. 3. Exposure to 7% CO_2 normalizes lung tissue macrophage number and tumor necrosis factor (TNF)-α content. Pups were treated from postnatal days 1–14 with vehicle (open bars) or bleomycin (1 mg·kg^{-1}·day^{-1}; closed bars) while receiving concurrent exposure to normocapnia (< 0.5%) or 5% or 7% CO_2. Representative medium-power photomicrographs of CD68-immunostaining (large dark brown cells highlighted by arrows; *A*) and isolectin B_4-labeled frozen sections (green fluorescent-labeled cells highlighted by arrows; *B*) demonstrating increased numbers of tissue macrophages in bleomycin-exposed animals (bleomycin), which was largely prevented by concurrent exposure to 7% CO_2 (bleomycin + 7% CO_2). Bar lengths = 100 μm. *C*: tissue macrophage and neutrophil counts per field normalized to tissue fraction. Values represent means ± SE for $n = 4$ animals/group. *D*: Western blot analyses of lung TNF-α content normalized to GAPDH. Representative immunoblots are shown with noncontiguous gel lanes demarcated by black lines. Values represent means ± SE for $n = 4$ samples/group. *$P < 0.01$, by one-way ANOVA, compared with vehicle-treated groups. #$P < 0.01$, by one-way ANOVA, compared with bleomycin-treated normocapnia-exposed group. *E*: representative photomicrographs of fluorescent immunolabeling for CD68 and TNF-α, demonstrating colocalization with tissue macrophages (bar length = 50 μm).

this cell type as the major source of TNF-α in the bleomycin-exposed lung.

Effects of TNF-α inhibition on bleomycin-induced pulmonary hypertension, macrophage influx, and abnormal distal lung morphology. Bleomycin-induced increases in PVR index, RVH and %MWT in pulmonary resistance arteries were all normalized by treatment with etanercept (Figs. 4, *A* and *B*), In contrast, treatment with etanercept had no effect on bleomycin-induced macrophage influx (Fig. 4*C*), indicating that upregulated TNF-α signaling does not contribute to increased numbers of activated tissue macrophages in the bleomycin-exposed lung. As shown in representative low-power hematoxylin and eosin-stained sections (Fig. 5*A*), abnormal lung morphology in bleomycin-treated animals was unaffected by treatment with etanercept, as evidenced by MLI, tissue fraction, secondary crest counts, and peripheral artery counts that did not differ ($P > 0.05$) from animals treated with bleomycin and vehicle (Fig. 5*B*).

Effects of bleomycin and/or 7% CO_2 on brain, liver, and kidney weights and on apoptosis in brain cortex. As shown in Table 4, exposure to bleomycin led to no change in brain or liver weight, while causing a small, but statistically significant ($P < 0.05$), decrease in combined kidney weight. Exposure to 7% CO_2 caused no change in brain, liver, or kidney weight in either vehicle- or bleomycin-treated animals (Table 4). In support of a lack of effect of a 14-day exposure to 7% CO_2 on brain growth, no apparent increase in TUNEL-labeled nuclei was observed compared with normocapnic controls (Fig. 6).

DISCUSSION

The effects of chronic CO_2 exposure on the neonatal lung and pulmonary vasculature have received limited attention in experimental models despite the widespread use of permissive hypercapnia in the newborn intensive care unit in the hope of limiting lung injury. We have previously shown that chronic inhalation of CO_2 prevented PHT in chronic hypoxia-exposed neonatal rats (31), a model in which pulmonary inflammation is not apparent (47). Given the major putative role for lung inflammation in the pathogenesis of BPD (61, 62, 66) and evidence for anti-inflammatory effects of inhaled CO_2 (37, 40, 45, 72), we were interested in examining the effects of therapeutic hypercapnia on an alternative rat model in which inflammation is a prominent early feature. The concentrations of CO_2 examined in bleomycin-exposed animals were intended to reproduce what are generally considered, in the clinical setting, to represent moderate (5% CO_2; mean elevation of Pa_{CO_2} 15–20 mmHg) and severe (7% CO_2; mean elevation of Pa_{CO_2} 35 mmHg) levels of hypercapnia. Our findings were that 7% CO_2 attenuated the hemodynamic and structural indexes of PHT secondary to bleomycin, whereas 5% CO_2 had lesser or no effects on these parameters. These changes were associated with attenuated tissue macrophage influx and TNF-α expression and content in the bleomycin-exposed lung. Our findings, which suggest a major role for tissue macrophages in the pathogenesis of chronic neonatal PHT, are in agreement with previous work from our group using a neonatal rat model of

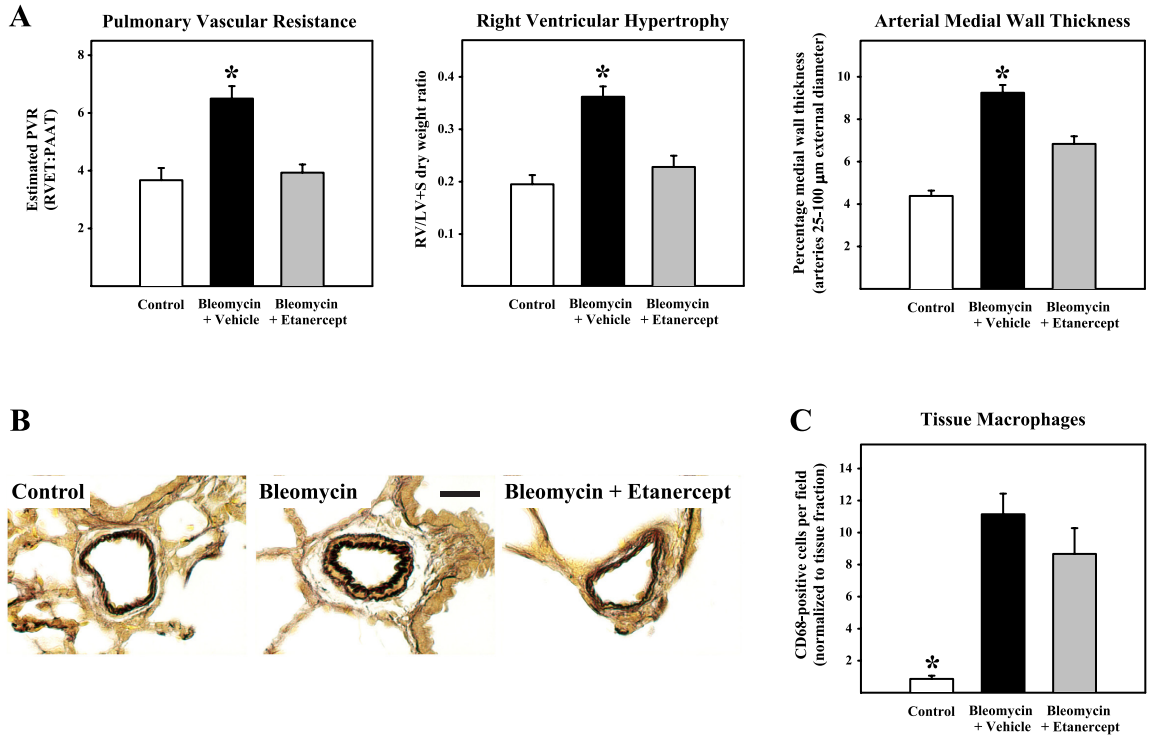

Fig. 4. TNF-α inhibition prevents bleomycin-induced pulmonary hypertension without affecting tissue macrophage number. Pups were treated from postnatal *days 1–14* with 0.9% saline vehicle (Control; open bars), bleomycin alone (1 mg·kg^{-1}·day^{-1}; closed bars) or bleomycin and etanercept (0.4 mg/kg ip alternate days; grey bars). All values represent means ± SE. *A*, *left*: PVR, as estimated by the RVET/PAAT ratio ($n = 6$ animals/group). *A*, *middle*: RV/LV + S dry weight ratios as a marker of right-ventricular hypertrophy ($n = 6$ animals/group). *A*, *right*: percentage arterial medial wall thickness as a marker of pulmonary arterial remodeling ($n = 3$–4 animals/group). *$P < 0.01$, by ANOVA, compared with all other groups. *B*: representative photomicrographs of elastin staining (dark brown inner and outer elastic laminae delineating the medial vascular wall; bar length = 25 μm) demonstrating medial wall thickening in bleomycin-exposed animals (bleomycin), which was prevented by treatment with etanercept (bleomycin + etanercept). *C*: tissue macrophage counts per field normalized to tissue fraction. Values represent means ± SE for $n = 4$ samples or animals/group. *$P < 0.01$, by ANOVA, compared with other groups.

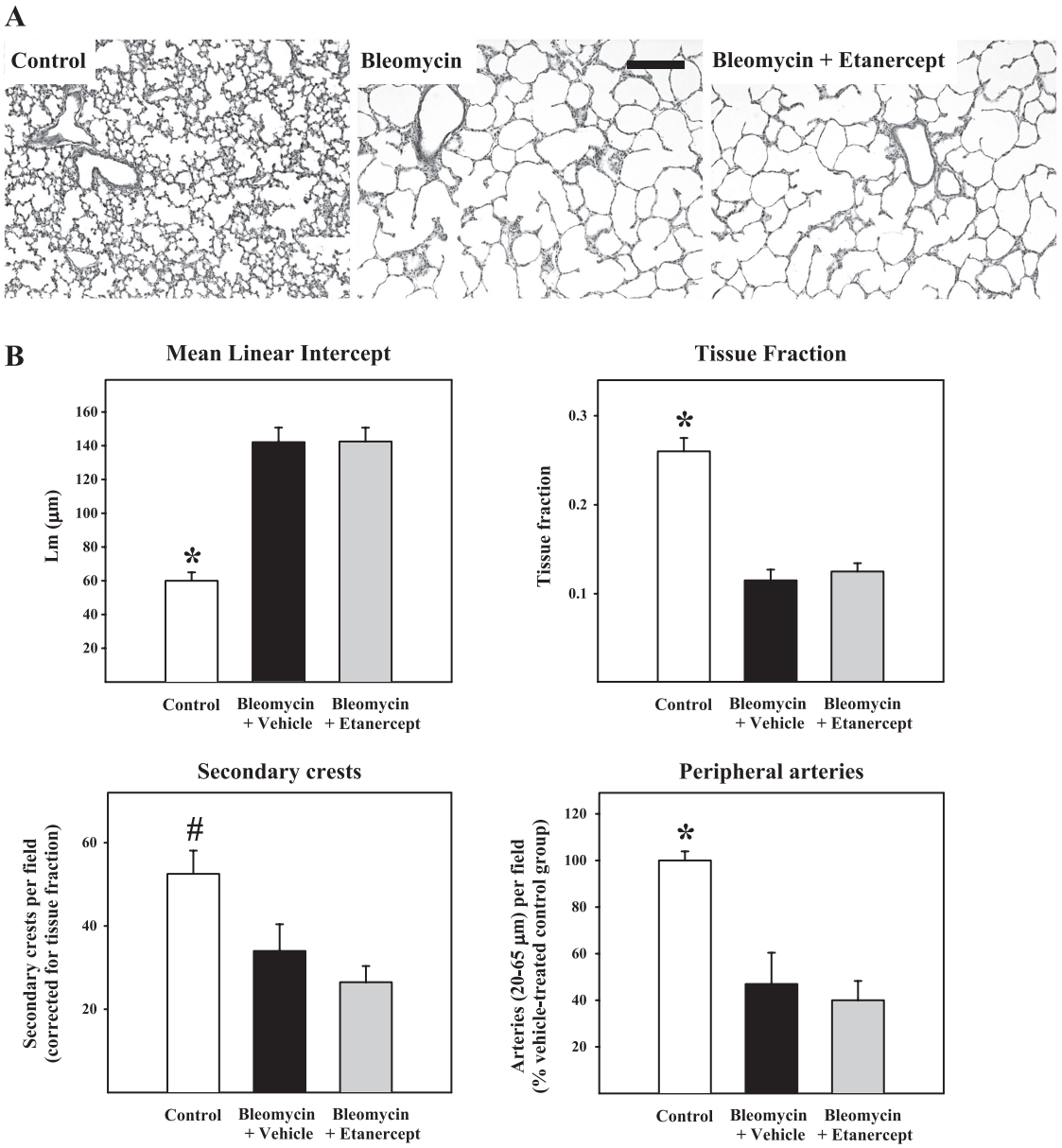

Fig. 5. TNF-α inhibition does not improve abnormal distal airway morphology. Pups were treated from postnatal *days 1–14* with 0.9% saline vehicle (Control; open bars), bleomycin alone (1 mg·kg^{-1}·day^{-1}; closed bars), or bleomycin and etanercept (0.4 mg/kg ip alternate days; grey bars). *A*: representative low-power photomicrographs of hematoxylin and eosin-stained sections demonstrating marked distal airway simplification and septal thinning in bleomycin-treated animals, which was unaffected by treatment with etanercept. Bar length = 200 μm. *B*: morphometric analyses of mean linear intercept (Lm), tissue fraction, and secondary crests or peripheral arteries per field, corrected for tissue fraction. Values represent means ± SE for $n = 4$ animals/group. *$P < 0.01$, by one-way ANOVA, compared with other groups. #$P < 0.05$, by one-way ANOVA, compared with other groups.

BPD secondary to hyperoxia (24), in which chronic inhalation of CO_2 was also shown to limit macrophage influx and to prevent the structural changes of PHT (45).

Examination of arterial acid-base status revealed that a 14-day exposure to 7% CO_2 caused significant acidosis, whereas 5% CO_2 did not, due in part to differing degrees of metabolic correction. A possible implication of these observations is that benefits of CO_2 were related to acidosis, rather than to hypercapnia, in keeping with recent findings in adult animals by Christou et al. (9). Furthermore, in short-term lung injury models, normalizing pH by buffering has been shown to worsen injury (36) where inhaled CO_2 has otherwise been protective (38, 64, 72). It was not possible to separate the effects of acidosis from hypercapnia by buffering in this chronic model, leaving the relative contributions of hypercapnia and acidosis an open question. Interestingly, both levels of hypercapnia increased Pa_{O_2} levels, in keeping with previously reported observations made by our group (31) and others (19, 35). Possible mechanisms for this effect include increased cardiac output, improved ventilation-perfusion matching, and reduced tissue metabolic activity and O_2 consumption (28).

Macrophages are differentiated mononuclear phagocytes that may reside in tissues for several months or be recruited to injured tissue from circulating monocytes, which then change phenotype. Although macrophages are essential for tissue remodeling and wound healing, when activated and present in

Table 4. *Brain, liver, and kidney weights on day 14*

Parameter/Group	Vehicle + Normocapnia	Bleomycin + Normocapnia	Vehicle + 7% CO_2	Bleomycin + 7% CO_2
Brain weight, mg	1,116 ± 39	1,080 ± 43	1,110 ± 21	1,083 ± 27
Brain weight/body weight × 10^3	35.5 ± 1.6	36.9 ± 1.4	34.4 ± 1.4	36.9 ± 1.8
Liver weight, mg	956 ± 68	960 ± 83	1033 ± 76	912 ± 24
Liver weight/body weight × 10^3	30.4 ± 1.7	32.8 ± 1.5	31.4 ± 2.0	30.7 ± 2.1
Kidney weights, mg	316 ± 22	290 ± 12	353 ± 30	260 ± 18*
Kidney weights/body weight × 10^3	10.1 ± 0.6	9.9 ± 0.3	10.7 ± 0.8	8.9 ± 0.8*

Values represent means ± SD; n = 5–6 animals per group. *$P < 0.01$, by ANOVA, compared with vehicle-treated 7% CO_2-exposed group.

exaggerated numbers, they may produce large quantities of reactive oxygen (34) and nitrogen (21, 45) species, bioactive lipid peroxidation products (75), and cytokines (60). In human preterm infants with respiratory distress, macrophage numbers in bronchoalveolar lavage fluid increase early in the second week of life (48), remain elevated in infants who later develop clinical and radiological features of BPD, and decline in those who do not (10). Pulmonary macrophages are also central to the pathogenesis of PHT induced by monocrotaline injection in rats (50, 70) and in anti-platelet serum-induced PHT in sheep (51). We remain uncertain whether increased tissue macrophages in the present model result from recruitment of circulating monocytes to the lung or whether they result from expansion of resident macrophages. However, our observation that expression of classical macrophage chemokines, including CCL2 (also known as monocyte chemoattractant protein-1), CCL3, and CCL4, were not increased in bleomycin-exposed animals suggests the latter possibility.

Of a number of cytokines screened to determine whether a causative role may exist, TNF-α was the only candidate found to be upregulated by bleomycin at the time point (*day 14*) examined. That both macrophage numbers and TNF-α expression/content were found to be attenuated by concurrent exposure to 7% CO_2 suggested a causative role in PHT, with a lesser effect of 5% CO_2 and colocalization indicating that macrophages were the major source of TNF-α. Lang et al. (39) have described inhibition of TNF-α secretion by CO_2 in pulmonary macrophages activated by LPS in vitro. Exogenous administration of TNF-α is also known to increase pulmonary vascular reactivity in isolated rat lungs (68), and its overexpression has been described to cause emphysematous lung structure and PHT in mice (16, 17), similar to bleomycin-induced lung injury. Furthermore, Sutendra et al. (71) recently reported that sustained inhibition of TNF-α signaling both prevented and reversed chronic PHT in monocrotaline-exposed rats. Similarly, a critical role for increased TNF-α signaling in PHT was confirmed in the present model using a soluble TNF-2 receptor/IgG fusion protein, etanercept, which prevents binding of the endogenous ligand to its receptors. Our group has used this approach successfully in the past to explore the roles of various growth factors in lung development and injury (8, 26). Our data do not provide insight into the downstream mediators of upregulated TNF-α signaling that led to PHT, but candidates implicated in other models include upregulation of endothelin-1 (43) and activation of Rho-kinase (46). Further, the upstream mechanisms causing a decrease in tissue macrophages by 7% CO_2 were also not elucidated in the present study; however, our data suggest there is no relationship

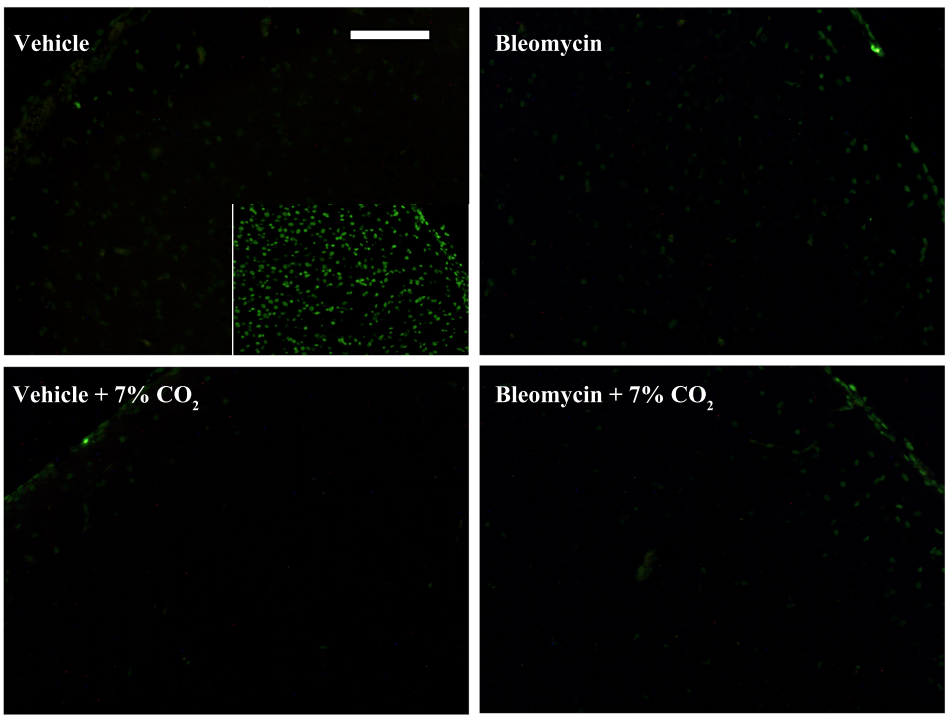

Fig. 6. Neither bleomycin nor exposure to 7% CO_2 increases apoptosis in brain cortex. Representative photomicrographs of terminal deoxyuridine triphosphate nick-end-labeled sections of brain cortex demonstrating no differences in numbers of apoptotic nuclei between groups. *Inset* (*top left*): DNAse I-treated positive control section. Bar length = 100 μm.

between inhibition of TNF-α and decrease in recruitment or activation of macrophages in the bleomycin-exposed lung.

In contrast with our previous findings in 60% O_2-exposed neonatal rats (45), therapeutic hypercapnia did not improve abnormal lung structure in the present model. Tourneux et al. (74) reported in bleomycin-exposed neonatal rats that inhaled nitric oxide prevented PHT and partially improved vascular rarefaction and lung structure, suggesting a major role for decreased endogenous NO. Our observation that PVR was normalized by 7% CO_2, while arterial rarefaction was not, suggests that vascular hypoplasia was not the major factor accounting for raised PVR. These findings are in keeping with our previous work (47) that demonstrated that acute treatment with a potent vasodilator (Rho-kinase inhibitor) also normalized PVR, thus pointing to sustained vasoconstriction as the major contributor to raised PVR in bleomycin-exposed animals, as described in other chronic PHT models (55).

We observed that neutrophils, which were greatly increased in number in the lung tissue of bleomycin-exposed animals, were unaffected by exposure to CO_2. These findings suggest that neutrophils alone are unlikely to be contributory to chronic PHT and that macrophages may not recruit neutrophils to the bleomycin-exposed lung. Indeed, work by others (73) suggests that neutrophils do not play a major role in bleomycin-induced lung injury, as least in adult animals, but our current observations leave open the question of their involvement in arrested lung development in the bleomycin-exposed neonatal rat. Although there are many other factors in the bleomycin model that could contribute to arrested development, neutrophils have been suggested to play a part by producing proteases that disrupt elastin deposition, which is essential to secondary septation (5).

We examined the effects of CO_2 on inflammation and lung structure in control (vehicle-treated) animals and observed small, but nonstatistically significant, trends toward increased inflammatory cells, decreased MLI, and decreased secondary crest numbers with 7% CO_2. In neonatal mice, chronic exposure to 8% CO_2 from birth has been reported to induce changes in lung morphology consistent with accelerated maturation, including thinning of alveolar walls and increased secondary septation (13). Taken together, these observations sound a note of caution that the risks vs. benefits of chronic hypercapnia for long-term lung development, function, and susceptibility to lung injury remain unclear and require further study. In addition, despite our present findings suggesting a lack of effect of 7% CO_2 on brain growth, there remains the potential for harmful effects of hypercapnia, or hypercapnic acidosis, on the immature brain (28, 30).

There are a number of limitations to this study. First, a major feature of bleomycin-induced lung injury is collagen deposition (32), which is not a feature of modern BPD (11). Our use of this model for the present studies was based on the striking degree of arrested lung growth and development, which is disproportionate to effects on other organs despite systemic administration, and the fact that macrophage influx, known to be involved in the pathogenesis of pulmonary hypertension, is a prominent early feature. Second, our estimation of arterial blood gases in anesthetized animals introduced the likelihood of respiratory suppression, which may have confounded data on Pa_{CO_2}, although we anticipate that all groups would have been affected equally. Our purpose in providing these data was to estimate the degree of change in Pa_{CO_2} and acid-base status secondary to provide some clinical context.

In conclusion, our current findings indicate that therapeutic hypercapnia has a dose-dependent preventive effect on chronic bleomycin-induced PHT relating to inhibitory effects on macrophage influx and subsequent attenuation of TNF-α. We propose that bleomycin-induced lung injury may represent a potentially useful new model for mechanistic studies relating to arrested development and chronic PHT in the neonatal lung.

GRANTS

This work was supported by operating funding from the Canadian Institutes of Health Research (CIHR; MOP-93956 to R. P. Jankov and MOP-82703 to A. K. Tanswell) and by infrastructure funding from the Canada Foundation for Innovation (to R. P. Jankov). R. P. Jankov is a CIHR New Investigator.

DISCLOSURES

No conflicts of interest, financial or otherwise are declared by the author(s).

AUTHOR CONTRIBUTIONS

Author contributions: A.C.P.S., A.K.T., and R.P.J. conception and design of research; A.C.P.S., C.K., J.I., A.H.L., A.M., and A.J. performed experiments; A.C.P.S., C.K., J.I., A.H.L., A.J., P.J.M., and R.P.J. analyzed data; A.C.P.S., A.J., P.J.M., A.K.T., and R.P.J. interpreted results of experiments; A.C.P.S., A.M., P.J.M., and R.P.J. prepared figures; A.C.P.S. drafted manuscript; A.C.P.S., C.K., J.I., A.H.L., A.M., A.J., P.J.M., A.K.T., and R.P.J. edited and revised manuscript; A.C.P.S., C.K., J.I., A.H.L., A.M., A.J., P.J.M., A.K.T., and R.P.J. approved final version of manuscript.

REFERENCES

1. **Abman SH, Groothius JR.** Pathophysiology and treatment of bronchopulmonary dysplasia. Current issues. *Pediatr Clin North Am* 41: 277–315., 1994.
2. **Abolhassani M, Guais A, Chaumet-Riffaud P, Sasco AJ, Schwartz L.** Carbon dioxide inhalation causes pulmonary inflammation. *Am J Physiol Lung Cell Mol Physiol* 296: L657–L665, 2009.
3. **Aguilar S, Scotton CJ, McNulty K, Nye E, Stamp G, Laurent G, Bonnet D, Janes SM.** Bone marrow stem cells expressing keratinocyte growth factor via an inducible lentivirus protects against bleomycin-induced pulmonary fibrosis. *PLos One* 4: e8013, 2009.
4. **Bancalari E, Claure N, Sosenko IR.** Bronchopulmonary dysplasia: changes in pathogenesis, epidemiology and definition. *Semin Neonatol* 8: 63–71, 2003.
5. **Bland RD, Ertsey R, Mokres LM, Xu L, Jacobson BE, Jiang S, Alvira CM, Rabinovitch M, Shinwell ES, Dixit A.** Mechanical ventilation uncouples synthesis and assembly of elastin and increases apoptosis in lungs of newborn mice. Prelude to defective alveolar septation during lung development? *Am J Physiol Lung Cell Mol Physiol* 294: L3–L14, 2008.
6. **Blom-Muilwijk MC, Vriesendorp R, Veninga TS, Hofstra W, Sleyfer DT, Wieringa RA, Konings AW.** Pulmonary toxicity after treatment with bleomycin alone or in combination with hyperoxia. Studies in the rat. *Br J Anaesth* 60: 91–97, 1988.
7. **Broccard AF, Hotchkiss JR, Vannay C, Markert M, Sauty A, Feihl F, Schaller MD.** Protective effects of hypercapnic acidosis on ventilator-induced lung injury. *Am J Respir Crit Care Med* 164: 802–806, 2001.
8. **Buch S, Han RN, Cabacungan J, Wang J, Yuan S, Belcastro R, Deimling J, Jankov R, Luo X, Lye SJ, Post M, Tanswell AK.** Changes in expression of platelet-derived growth factor and its receptors in the lungs of newborn rats exposed to air or 60% O_2. *Pediatr Res* 48: 423–433, 2000.
9. **Christou H, Reslan OM, Mam V, Tanbe AF, Vitali SH, Touma M, Arons E, Mitsialis SA, Kourembanas S, Khalil RA.** Improved pulmonary vascular reactivity and decreased hypertrophic remodeling during non-hypercapnic acidosis in experimental pulmonary hypertension. *Am J Physiol Lung Cell Mol Physiol* 302: L875–L890, 2012.
10. **Clement A, Chadelat K, Sardet A, Grimfeld A, Tournier G.** Alveolar macrophage status in bronchopulmonary dysplasia. *Pediatr Res* 23: 470–473, 1988.
11. **Coalson JJ.** Pathology of new bronchopulmonary dysplasia. *Semin Neonatol* 8: 73–81, 2003.

12. **Cutroneo KR, White SL, Phan SH, Ehrlich HP.** Therapies for bleomycin induced lung fibrosis through regulation of TGF-beta1 induced collagen gene expression. *J Cell Physiol* 211: 585–589, 2007.
13. **Das S, Du Z, Bassly S, Singer L, Vicencio AG.** Effects of chronic hypercapnia in the neonatal mouse lung and brain. *Pediatr Pulmonol* 44: 176–182, 2009.
14. **De Smet HR, Bersten AD, Barr HA, Doyle IR.** Hypercapnic acidosis modulates inflammation, lung mechanics, and edema in the isolated perfused lung. *J Crit Care* 22: 305–313, 2007.
15. **Farquhar M, Fitzgerald DA.** Pulmonary hypertension in chronic neonatal lung disease. *Paediatr Respir Rev* 11: 149–153, 2010.
16. **Fujita M, Mason RJ, Cool C, Shannon JM, Hara N, Fagan KA.** Pulmonary hypertension in TNF-α-overexpressing mice is associated with decreased VEGF gene expression. *J Appl Physiol* 93: 2162–2170, 2002.
17. **Fujita M, Shannon JM, Irvin CG, Fagan KA, Cool C, Augustin A, Mason RJ.** Overexpression of tumor necrosis factor-α produces an increase in lung volumes and pulmonary hypertension. *Am J Physiol Lung Cell Mol Physiol* 280: L39–L49, 2001.
18. **Gazoni LM, Tribble CG, Zhao MQ, Unger EB, Farrar RA, Ellman PI, Fernandez LG, Laubach VE, Kron IL.** Pulmonary macrophage inhibition and inhaled nitric oxide attenuate lung ischemia-reperfusion injury. *Ann Thorac Surg* 84: 247–253, 2007.
19. **Gharaee-Kermani M, McCullumsmith RE, Charo IF, Kunkel SL, Phan SH.** CC-chemokine receptor 2 required for bleomycin-induced pulmonary fibrosis. *Cytokine* 24: 266–276, 2003.
20. **Hagimoto N, Kuwano K, Nomoto Y, Kunitake R, Hara N.** Apoptosis and expression of Fas/Fas ligand mRNA in bleomycin-induced pulmonary fibrosis in mice. *Am J Respir Cell Mol Biol* 16: 91–101, 1997.
21. **Ischiropoulos H, Zhu L, Beckman JS.** Peroxynitrite formation from macrophage-derived nitric oxide. *Arch Biochem Biophys* 298: 446–451, 1992.
22. **Jankov RP, Kantores C, Belcastro R, Yi M, Tanswell AK.** Endothelin-1 inhibits apoptosis of pulmonary arterial smooth muscle in the neonatal rat. *Pediatr Res* 60: 245–251, 2006.
23. **Jankov RP, Kantores C, Belcastro R, Yi S, Ridsdale RA, Post M, Tanswell AK.** A role for platelet-derived growth factor β-receptor in a newborn rat model of endothelin-mediated pulmonary vascular remodeling. *Am J Physiol Lung Cell Mol Physiol* 288: L1162–L1170, 2005.
24. **Jankov RP, Luo X, Belcastro R, Copland I, Frndova H, Lye SJ, Hoidal JR, Post M, Tanswell AK.** Gadolinium chloride inhibits pulmonary macrophage influx and prevents O_2-induced pulmonary hypertension in the neonatal rat. *Pediatr Res* 50: 172–183, 2001.
25. **Jankov RP, Luo X, Cabacungan J, Belcastro R, Frndova H, Lye SJ, Tanswell AK.** Endothelin-1 and O_2-mediated pulmonary hypertension in neonatal rats: a role for products of lipid peroxidation. *Pediatr Res* 48: 289–298, 2000.
26. **Jankov RP, Luo X, Campbell A, Belcastro R, Cabacungan J, Johnstone L, Frndova H, Lye SJ, Tanswell AK.** Fibroblast growth factor receptor-1 and neonatal compensatory lung growth after exposure to 95% oxygen. *Am J Respir Crit Care Med* 167: 1554–1561, 2003.
27. **Jankov RP, Luo X, Demin P, Aslam R, Hannam V, Tanswell AK, Pace-Asciak CR.** Hepoxilin analogs inhibit bleomycin-induced pulmonary fibrosis in the mouse. *J Pharmacol Exp Ther* 301: 435–440, 2002.
28. **Jankov RP, Tanswell AK.** Hypercapnia and the neonate. *Acta Paediatr* 97: 1502–1509, 2008.
29. **Jobe AJ.** The new BPD: an arrest of lung development. *Pediatr Res* 46: 641–643, 1999.
30. **Kaiser JR, Gauss CH, Williams DK.** The effects of hypercapnia on cerebral autoregulation in ventilated very low birth weight infants. *Pediatr Res* 58: 931–935, 2005.
31. **Kantores C, McNamara PJ, Teixeira L, Engelberts D, Murthy P, Kavanagh BP, Jankov RP.** Therapeutic hypercapnia prevents chronic hypoxia-induced pulmonary hypertension in the newborn rat. *Am J Physiol Lung Cell Mol Physiol* 291: L912–L922, 2006.
32. **Kelley J, Newman RA, Evans JN.** Bleomycin-induced pulmonary fibrosis in the rat. Prevention with an inhibitor of collagen synthesis. *J Lab Clin Med* 96: 954–964, 1980.
33. **Khemani E, McElhinney DB, Rhein L, Andrade O, Lacro RV, Thomas KC, Mullen MP.** Pulmonary artery hypertension in formerly premature infants with bronchopulmonary dysplasia: clinical features and outcomes in the surfactant era. *Pediatrics* 120: 1260–1269, 2007.
34. **Kinnula VL, Chang LY, Ho YS, Crapo JD.** Hydrogen peroxide release from alveolar macrophages and alveolar type II cells during adaptation to hyperoxia in vivo. *Exp Lung Res* 18: 655–673, 1992.
35. **Kregenow DA, Swenson ER.** The lung and carbon dioxide: implications for permissive and therapeutic hypercapnia. *Eur Respir J* 20: 6–11, 2002.
36. **Laffey JG, Engelberts D, Kavanagh BP.** Buffering hypercapnic acidosis worsens acute lung injury. *Am J Respir Crit Care Med* 161: 141–146, 2000.
37. **Laffey JG, Honan D, Hopkins N, Hyvelin JM, Boylan JF, McLoughlin P.** Hypercapnic acidosis attenuates endotoxin-induced acute lung injury. *Am J Respir Crit Care Med* 169: 46–56, 2004.
38. **Laffey JG, Tanaka M, Engelberts D, Luo X, Yuan S, Tanswell AK, Post M, Lindsay T, Kavanagh BP.** Therapeutic hypercapnia reduces pulmonary and systemic injury following in vivo lung reperfusion. *Am J Respir Crit Care Med* 162: 2287–2294, 2000.
39. **Lang CJ, Dong P, Hosszu EK, Doyle IR.** Effect of CO_2 on LPS-induced cytokine responses in rat alveolar macrophages. *Am J Physiol Lung Cell Mol Physiol* 289: L96–L103, 2005.
40. **Li G, Zhou D, Vicencio AG, Ryu J, Xue J, Kanaan A, Gavrialov O, Haddad GG.** Effect of carbon dioxide on neonatal mouse lung: a genomic approach. *J Appl Physiol* 101: 1556–1564, 2006.
41. **MacCarrick MJ, Torbati D, Kimura D, Raszynski A, Zeng W, Totapally BR.** Does hypercapnia ameliorate hyperoxia-induced lung injury in neonatal rats? *Lung* 188: 235–240, 2010.
42. **Maddox DE, Shibata S, Goldstein IJ.** Stimulated macrophages express a new glycoprotein receptor reactive with Griffonia simplicifolia I-B4 isolectin. *Proc Natl Acad Sci USA* 79: 166–170, 1982.
43. **Marsden PA, Brenner BM.** Transcriptional regulation of the endothelin-1 gene by TNF-α. *Am J Physiol Cell Physiol* 262: C854–C861, 1992.
44. **Masood A, Belcastro R, Li J, Kantores C, Jankov RP, Tanswell AK.** A peroxynitrite decomposition catalyst prevents 60% O_2-mediated rat chronic neonatal lung injury. *Free Radic Biol Med* 49: 1182–1191, 2010.
45. **Masood A, Yi M, Lau M, Belcastro R, Shek S, Pan J, Kantores C, McNamara PJ, Kavanagh BP, Belik J, Jankov RP, Tanswell AK.** Therapeutic effects of hypercapnia on chronic lung injury and vascular remodeling in neonatal rats. *Am J Physiol Lung Cell Mol Physiol* 297: L920–L930, 2009.
46. **Matoba K, Kawanami D, Ishizawa S, Kanazawa Y, Yokota T, Utsunomiya K.** Rho-kinase mediates TNF-α-induced MCP-1 expression via p38 MAPK signaling pathway in mesangial cells. *Biochem Biophys Res Commun* 402: 725–730, 2010.
47. **McNamara PJ, Murthy P, Kantores C, Teixeira L, Engelberts D, van Vliet T, Kavanagh BP, Jankov RP.** Acute vasodilator effects of Rho-kinase inhibitors in neonatal rats with pulmonary hypertension unresponsive to nitric oxide. *Am J Physiol Lung Cell Mol Physiol* 294: L205–L213, 2008.
48. **Merritt TA, Stuard ID, Puccia J, Wood B, Edwards DK, Finkelstein J, Shapiro DL.** Newborn tracheal aspirate cytology: classification during respiratory distress syndrome and bronchopulmonary dysplasia. *J Pediatr* 98: 949–956, 1981.
49. **Miller JD, Carlo WA.** Safety and effectiveness of permissive hypercapnia in the preterm infant. *Curr Opin Pediatr* 19: 142–144, 2007.
50. **Miyata M, Sakuma F, Yoshimura A, Ishikawa H, Nishimaki T, Kasukawa R.** Pulmonary hypertension in rats. 1. Role of bromodeoxyuridine-positive mononuclear cells and alveolar macrophages. *Int Arch Allergy Immunol* 108: 281–286, 1995.
51. **Nakano T, Miyamoto K, Nishimura M, Aida A, Aoi K, Kawakami Y.** Role of pulmonary intravascular macrophages in anti-platelet serum-induced pulmonary hypertension in sheep. *Respir Physiol* 98: 83–99, 1994.
52. **Nichol AD, O'Cronin DF, Naughton F, Hopkins N, Boylan J, McLoughlin P.** Hypercapnic acidosis reduces oxidative reactions in endotoxin-induced lung injury. *Anesthesiology* 113: 116–125, 2010.
53. **Norozian FM, Leoncio M, Torbati D, Meyer K, Raszynski A, Totapally BR.** Therapeutic hypercapnia enhances the inflammatory response to endotoxin in the lung of spontaneously breathing rats. *Crit Care Med* 39: 1400–1406, 2011.
54. **O'Croinin DF, Nichol AD, Hopkins N, Boylan J, O'Brien S, O'Connor C, Laffey JG, McLoughlin P.** Sustained hypercapnic acidosis during pulmonary infection increases bacterial load and worsens lung injury. *Crit Care Med* 36: 2128–2135, 2008.
55. **Oka M, Fagan KA, Jones PL, McMurtry IF.** Therapeutic potential of RhoA/Rho kinase inhibitors in pulmonary hypertension. *Br J Pharmacol* 155: 444–454, 2008.
56. **Ooi H, Cadogan E, Sweeney M, Howell K, O'Regan RG, McLoughlin P.** Chronic hypercapnia inhibits hypoxic pulmonary vascular remodeling. *Am J Physiol Heart Circ Physiol* 278: H331–H338, 2000.

57. **Padela S, Cabacungan J, Shek S, Belcastro R, Yi M, Jankov RP, Tanswell AK.** Hepatocyte growth factor is required for alveologenesis in the neonatal rat. *Am J Respir Crit Care Med* 172: 907–914, 2005.
58. **Parker TA, Abman SH.** The pulmonary circulation in bronchopulmonary dysplasia. *Semin Neonatol* 8: 51–61, 2003.
59. **Pendino KJ, Meidhof TM, Heck DE, Laskin JD, Laskin DL.** Inhibition of macrophages with gadolinium chloride abrogates ozone-induced pulmonary injury and inflammatory mediator production. *Am J Respir Cell Mol Biol* 13: 125–132, 1995.
60. **Pendino KJ, Shuler RL, Laskin JD, Laskin DL.** Enhanced production of interleukin-1, tumor necrosis factor-α, and fibronectin by rat lung phagocytes following inhalation of a pulmonary irritant. *Am J Respir Cell Mol Biol* 11: 279–286, 1994.
61. **Pierce MR, Bancalari E.** The role of inflammation in the pathogenesis of bronchopulmonary dysplasia. *Pediatr Pulmonol* 19: 371–378, 1995.
62. **Ryan RM, Ahmed Q, Lakshminrusimha S.** Inflammatory mediators in the immunobiology of bronchopulmonary dysplasia. *Clin Rev Allergy Immunol* 34: 174–190, 2008.
63. **Sato S, Kato S, Arisaka Y, Takahashi H, Takahashi K, Tomoike H.** Changes in pulmonary hemodynamics during normoxia and hypoxia in awake rats treated with intratracheal bleomycin. *Tohoku J Exp Med* 169: 233–244, 1993.
64. **Shibata K, Cregg N, Engelberts D, Takeuchi A, Fedorko L, Kavanagh BP.** Hypercapnic acidosis may attenuate acute lung injury by inhibition of endogenous xanthine oxidase. *Am J Respir Crit Care Med* 158: 1578–1584, 1998.
65. **Sinclair SE, Kregenow DA, Lamm WJ, Starr IR, Chi EY, Hlastala MP.** Hypercapnic acidosis is protective in an in vivo model of ventilator-induced lung injury. *Am J Respir Crit Care Med* 166: 403–408, 2002.
66. **Speer CP.** Inflammation and bronchopulmonary dysplasia. *Semin Neonatol* 8: 29–38, 2003.
67. **Steinhorn RH.** Neonatal pulmonary hypertension. *Pediatr Crit Care Med* 11: S79–S84, 2010.
68. **Stevens T, Janssen PL, Tucker A.** Acute and long-term TNF-α administration increases pulmonary vascular reactivity in isolated rat lungs. *J Appl Physiol* 73: 708–712, 1992.
69. **Strand M, Ikegami M, Jobe AH.** Effects of high PCO_2 on ventilated preterm lamb lungs. *Pediatr Res* 53: 468–472, 2003.
70. **Sugita T, Stenmark KR, Wagner WW Jr, Henson PM, Henson JE, Hyers TM, Reeves JT.** Abnormal alveolar cells in monocrotaline induced pulmonary hypertension. *Exp Lung Res* 5: 201–215, 1983.
71. **Sutendra G, Dromparis P, Bonnet S, Haromy A, McMurtry MS, Bleackley RC, Michelakis ED.** Pyruvate dehydrogenase inhibition by the inflammatory cytokine TNFα contributes to the pathogenesis of pulmonary arterial hypertension. *J Mol Med* 89: 771–783, 2011.
72. **Takeshita K, Suzuki Y, Nishio K, Takeuchi O, Toda K, Kudo H, Miyao N, Ishii M, Sato N, Naoki K, Aoki T, Suzuki K, Hiraoka R, Yamaguchi K.** Hypercapnic acidosis attenuates endotoxin-induced nuclear factor-κB activation. *Am J Respir Cell Mol Biol* 29: 124–132, 2003.
73. **Thrall RS, Phan SH, McCormick JR, Ward PA.** The development of bleomycin-induced pulmonary fibrosis in neutrophil-depleted and complement-depleted rats. *Am J Pathol* 105: 76–81, 1981.
74. **Tourneux P, Markham N, Seedorf G, Balasubramaniam V, Abman SH.** Inhaled nitric oxide improves lung structure and pulmonary hypertension in a model of bleomycin-induced bronchopulmonary dysplasia in neonatal rats. *Am J Physiol Lung Cell Mol Physiol* 297: L1103–L1111, 2009.
75. **Vacchiano CA, Osborne GR, Tempel GE.** 8-iso-PGF2a production by alveolar macrophages exposed to hyperoxia. *Shock* 9: 266–273, 1998.
76. **van Kaam AH, Rimensberger PC.** Lung-protective ventilation strategies in neonatology: what do we know-what do we need to know? *Crit Care Med* 35: 925–931, 2007.
77. **Williams JH Jr, Bodell P, Hosseini S, Tran H, and Baldwin KM.** Haemodynamic sequelae of pulmonary fibrosis following intratracheal bleomycin in rats. *Cardiovasc Res* 26: 401–408, 1992.